Hydrodechlorination of Tetrachloromethane over Palladium Catalysts Supported on Mixed MgF$_2$-MgO Carriers

Magdalena Bonarowska [1], Maria Wojciechowska [2], Maciej Zieliński [1], Angelika Kiderys [2], Michał Zieliński [2], Piotr Winiarek [3] and Zbigniew Karpiński [4],*

[1] Institute of Physical Chemistry, Polish Academy of Sciences, Kasprzaka 44/52, Warsaw 01-224, Poland; mbonarowska@ichf.edu.pl (M.B.); mzielinski@ichf.edu.pl (M.Z.)

[2] Faculty of Chemistry, Adam Mickiewicz University, Umultowska 89b, Poznań 61-614, Poland; emawoj@amu.edu.pl (M.W.); angelika.kiderys@gmail.com (A.K.); mardok@amu.edu.pl (M.Z.)

[3] Faculty of Chemistry, Warsaw University of Technology, Noakowskiego 3, Warsaw 00-664, Poland; piotrw@ch.pw.edu.pl

[4] Faculty of Mathematics and Natural Sciences, School of Science, Cardinal Stefan Wyszyński University, Wóycickiego 1/3, Warsaw 01-938, Poland

* Correspondence: z.karpinski@uksw.edu.pl; Tel.: +48-22-380-9624; Fax: +48-22-561-8902

Abstract: Pd/MgO, Pd/MgF$_2$ and Pd/MgO-MgF$_2$ catalysts were investigated in the reaction of CCl$_4$ hydrodechlorination. All the catalysts deactivated in time on stream, but the degree of deactivation varied from catalyst to catalyst. The MgF$_2$-supported palladium with relatively large metal particles appeared the best catalyst, characterized by good activity and selectivity to C$_2$-C$_5$ hydrocarbons. Investigation of post-reaction catalyst samples allowed to find several details associated with the working state of hydrodechlorination catalysts. The role of support acidity was quite complex. On the one hand, a definite, although not very high Lewis acidity of MgF$_2$ is beneficial for shaping high activity of palladium catalysts. The MgO-MgF$_2$ support characterized by stronger Lewis acidity than MgF$_2$ contributes to very good catalytic activity for a relatively long reaction period (~5 h) but subsequent neutralization of stronger acid centers (by coking) eliminates them from the catalyst. On the other hand, the role of acidity evolution, which takes place when basic supports (like MgO) are chlorided during HdCl reactions, is difficult to assess because different events associated with distribution of chlorided support species, leading to partial or even full blocking of the surface of palladium, which plays the role of active component in HdCl reactions.

Keywords: CCl$_4$ hydrodechlorination; palladium; MgF$_2$; MgO; MgO-MgF$_2$; supports; Lewis acidity

1. Introduction

Catalytic hydrodehalogenation (HdCl) of harmful organic compounds, such chloromethanes, CFCs or chlorobenzenes on supported metal catalysts, appear a useful method for transforming those detrimental compounds into valuable chemicals [1,2]. The active phase of these catalysts are metals, among which the best performance show platinum, palladium and nickel [2–5]. Recently published review article by Colombo et al. [6] highlights the suitability of iron catalysts in removing chlorocarbons from the water. In addition, the performance of the iron in water decontamination can be greatly improved by doping with other metals such as palladium, copper, silver and nickel. Besides, the role of support should not only be considered as a metal redispersing medium. Carbon is the support of industrial choice for a number of reasons, including high specific surface area and stability against corrosion by halogen-containing products of hydrodehalogenation (HCl, HF). Research with the use

of other supports, such as silica, alumina, zeolites or magnesia, served mainly for short-term model studies, when the functioning of various metallic phases is tested. The role of acido-basic properties of a support is not well understood, although several suggestions were made in this respect. Studied in the reaction of hydrodechlorination of 1,1-dichlorotetrafluoroethane, Pd catalysts supported on AlF_3 and MgF_2 (characterized by very dissimilar acidities) did not show large differences in their catalytic behavior [7]. It would speak against any special effect of support acidity on the hydrodechlorination performance. However, it is also known that the acidic or basic character of the support would modify metal particles, making them electrodeficient or electron-rich. The electron deficiency was found to depend on the concentration and the location of Brønsted acid sites [8]. Such effect would lead to a weaker interaction of the metal with reaction intermediates contributing to higher activities and product selectivities to, frequently desired, partly dehalogenated compounds [5,9]. Similarly, optimal combination of $Pd^{\sigma+}$ and Pd° species has recently been invoked for the best hydrodechlorination performance [10,11]. Electrodeficient palladium, Pd^{2+}, has been reported to improve the activity of Pd catalysts in HdCl reactions [12–17].

On the other hand, the presence of support acid centers would also lead to accumulation of polymeric species and catalyst's fouling by coking [18,19]. Less acidic supports would act as chlorine "sink", keeping the metal surface clean for a considerable time of reaction. This does not seem to function for highly acidic supports which, in addition, produce polymeric species, which in turn would be spilt over onto the metal surface [18].

In this respect, advantages of MgO as appropriate support of the hydrodechlorination catalyst are presented by several authors [20–22]. The high activity of the Pt/MgO catalyst was ascribed to basic properties of MgO. The basicity of this oxide seems to be responsible for retarding the coke formation and suppression of C_2 oligomers (C_2Cl_4 and C_2Cl_6 mainly) which are the principal reasons for the catalyst deactivation. Clarke et al. [23] studied MgO-supported Pt catalysts in the hydrogenolysis of C_5-C_6 hydrocarbons and came to conclusion that large changes in the catalytic behavior of platinum result from negative charge from the magnesia O^{2-} ions to the metal.

Suitability of MgF_2-supported metal catalysts for HdCl reactions was proved in numerous studies [7,14,20,21,24–28]. Because of a variety of investigated reactants, metal precursors (metal salts vs. phosphine complexes of metals, [28]), metal dispersion and structural forms of MgF_2 (high surface area form [26] vs. well-crystalline [25]) it difficult to describe shortly this issue in much detail. However, a general overview appears to appreciate very good overall activity, selectivity to desired products and stability of MgF_2-supported metals, usually exceeding the performance of their counterparts supported on oxidic carriers. The most often explanation takes into account the beneficial effect of MgF_2 on metal centers making them electrodeficient. $MgO \rightarrow MgF_2$ transformation during HdCl of CFCs over MgO-supported metals was also considered as important in shaping the active form of metal catalysts [29].

We have decided to study the hydrodechlorination of CCl_4 carried out over palladium catalysts supported on MgO-MgF_2 carriers, in strong belief that the acido-basic properties of these mixed materials are well correlated with their composition. By increasing the fluorine content of the magnesium oxide fluoride, the Lewis acidity increases whereas the basicity decreases [30]. Therefore, these sites can be tuned over a wide range of MgO-MgF_2 composition thus giving access to optimized catalytic activity and selectivity of these phases as was found for Michael additions [31]. However, during any hydrochlorination reactions which produce HCl the problem becomes more complicated. The reaction leads to a rapid transformation of MgO into $MgCl_2$ [20,21], which has to be considered in description of a working state of the Pd/MgO-MgF_2 catalyst. Full or even partial replacement of MgO by $MgCl_2$ should also result in an increase in the strength of Lewis acid sites on the surface of the catalyst.

2. Results and Discussion

2.1. Catalyst Characterization

Characterization of prepared MgO-MgF$_2$ carriers was reported in earlier publications, the "sol-gel" series in [32] and the "carbonate" series in [33] and are recalled in Table 1. For the "sol-gel" series, the content of magnesium oxide had a considerable effect on the surface area of the MgO-MgF$_2$ systems, i.e., the surface area of MgO-MgF$_2$ was seven times larger than that of pure magnesium fluoride and still larger than that of pure MgO. All the "sol-gel" samples were mesoporous with the mean pore diameters ranging from 8 to 18 nm. The size of the pores strongly depended on the composition of the samples and declined with increasing MgO content in MgO-MgF$_2$ samples. For the "carbonate" series the surface area of the mixed MgO-MgF$_2$ supports was 2–3 times greater than that of pure MgF$_2$. In general, the surface area of mixed supports increased with increasing amount of MgO introduced. The BET surface area of MgO was almost five times greater than that of MgF$_2$. All the "carbonate" series samples were mesoporous with the mean pore diameters ranging from 8 to 24 nm. The XRD studies showed the presence of separate crystalline MgO and MgF$_2$ phases [33].

Table 1. Support characterization (adapted from [32,33]).

Support	BET Surface Area (m$^2 \cdot$g^{-1})	Average Pore Diameter (nm)	Pore Volume (cm$^3 \cdot$g^{-1})
Sol-Gel Series			
MgO	152	10.5	0.39
62% MgO-38% MgF$_2$	208	8.2	0.43
33% MgO-67% MgF$_2$	144	17.8	0.64
MgF$_2$	32	15.5	0.12
Carbonate Series			
MgO	142.7	8.19	0.29
37% MgO-63% MgF$_2$	51.0	23.79	0.30
MgF$_2$	32.0	21.26	0.17

The present sample characterization concerns only the Pd-loaded MgO-MgF$_2$ catalysts, with attention focused on the metal component which is commonly regarded as the active phase in hydrodechlorination reactions. Table 2 shows metal dispersion data based on H$_2$ and CO chemisorptions. Considering the methodological (pulse vs. static) differences, the results obtained are internally consistent. In addition, the TPHD studies (Table 2) show larger H/Pd ratios for poorly dispersed palladium catalysts, in agreement with known correlations [34–36]. In the absence of XPS studies, these results would suggest that our palladium material reduced at 380 °C has not been significantly chemically modified by possible interactions with MgO-MgF$_2$ supports.

However, it is found that introduction of a larger amount of palladium (3%) onto a support characterized by a smaller surface area and lower pore volume (here MgF$_2$) results in the formation of relatively large Pd particles, i.e., ~8 nm (as assessed from CO chemisorption) compared to very small (~2 nm or less) metal particles deposited on MgO and MgO-MgF$_2$ carriers. It appears that the support of less developed pore structure is not able accommodate larger amounts of dissolved metal precursor during impregation whereas a highly developed pore structure leads to evenly distributed small portions of the precursor. More important is that such large difference in metal dispersion makes a direct comparison of catalytic pattern in these series difficult. Fortunately, smaller differences in surface areas in the "carbonate" series of MgO-MgF$_2$ supports and lower palladium loadings employed (1% instead of 3%) allowed to prepare the catalysts characterized by comparable metal dispersions (Table 2).

Table 2. Characteristics of Pd/MgO-MgF$_2$ catalysts: palladium dispersion and H/Pd ratio from Temperature Programmed Hydride Decomposition (TPHD).

Support Series [a]	Catalyst	H$_{ad}$/Pd From Pulse Chemisorption and Metal Particle Size (d, nm) [b]	CO$_{ad}$/Pd From Static Chemisorption and Metal Particle Size (d, nm) [c]	H/Pd From TPHD
sol-gel	3% Pd/MgO	0.509 (2.2)	0.661 (1.7)	0.12
	3% Pd/62% MgO-38% MgF$_2$	0.495 (2.3)	0.645 (1.7)	0.13
	3% Pd/33% MgO-67% MgF$_2$	0.554 (2.0)	0.672 (1.7)	0.11
	3% Pd/MgF$_2$	0.175 (6.4)	0.141 (7.9)	0.30
carbonate	3% Pd/MgO	0.647 (1.7)	0.633 (1.8)	0.11
	3% Pd/MgF$_2$	0.098 (11.4)	0.072 (15.6)	0.35
carbonate	1% Pd/MgO	n.m. [d]	0.323 (3.5)	n.m. [d]
	1% Pd/37% MgO-63% MgF$_2$	n.m. [d]	0.317 (3.5)	n.m. [d]
	1% Pd/MgF$_2$	n.m. [d]	0.259 (4.3)	n.m. [d]

[a] For support preparation and description, see subsection 3.1. [b] From pulse chemisorption of H$_2$ at 70 °C. Numbers in the parentheses indicate mean sizes of palladium particles calculated from the formula d$_{nm}$ = 1.12/(H$_{ad}$/Pd) [37]. [c] From static chemisorption of CO at 35 °C, taken for TOF calculation. Numbers in the parentheses indicate mean sizes of palladium particles calculated from the formula d$_{nm}$ = 1.12/(CO$_{ad}$/Pd). [d] Not measured.

The results of XRD studies of reduced 3 wt % Pd/MgO-MgF$_2$ catalysts are presented in Figure 1. A variety of large diffraction peaks from crystalline phases of MgO and MgF$_2$, overlapping reflections from highly dispersed palladium, prevent identification of the metal. Only in the case of 3 wt % Pd/MgF catalysts, the (200) reflection from the Pd (fcc phase) of low intensity would be identified. Rough estimation of Pd crystallite size from that reflection (using the Scherrer formulae) gives 12–15 nm, i.e., the value in a limited agreement with the Pd particle sizes assessed from chemisorption (Table 1). Accordingly, the diffractograms of the less metal loaded (1 wt %) Pd/MgO-MgF$_2$ catalysts resemble very much the profiles of unloaded supports [33], although a very small (200) reflection from palladium was also detected in the profile of the 1 wt % Pd/MgF$_2$ (XRD data not shown).
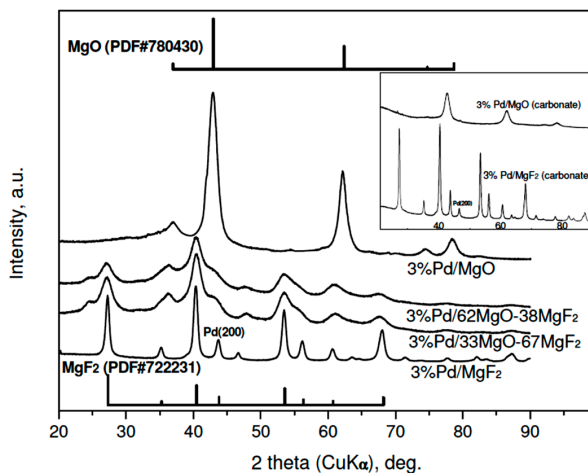
Figure 1. XRD profiles of reduced 3 wt % Pd/MgO-MgF$_2$ catalysts ("sol-gel" series). Reflections for MgF$_2$ and MgO are presented by bars proportional to their relative intensities. Inset: diffractograms of 3 wt % Pd catalysts of the "carbonate" series. To simplify the notation the composition of MgO-MgF$_2$ mixture the % symbol is usually dropped in further text.

2.2. Catalytic Performance of Pd/MgO-MgF$_2$ in CCl$_4$ Hydrodechlorination

2.2.1. Catalytic Activity

All tested Pd/MgO-MgF$_2$ catalysts deactivated during the hydrodechlorination of CCl$_4$ at 90 °C, but the character of deactivation varied between different samples.

Reasons for deactivation of HdCl metal catalysts were analyzed in previous publications. They are considered as metal surface chloriding by a liberated HCl [38–41], massive deposition of carbonaceous deposits on metal surface [42–45] and metal sintering caused by long-term operation [46]. It was rather well established that smaller Pd particles (~2 nm or less) deactivate faster than larger Pd crystalllites (~10 nm in size) [36]. Accordingly, our magnesia-containing Pd samples in the sol-gel series which are characterized by very small metal particles (Table 2) showed very pronounced deactivation during kinetic runs and low final activity (Figure 2). On the other hand, the superior catalytic performance, with a small decrease of conversion (from ~100% to ~93%) showed the 3 wt. % Pd/MgF$_2$ catalysts (sol-gel series), characterized by poor metal dispersion. Its counterpart from the carbonate series also exhibited high conversion, but a marked deactivation was observed in this case (from ~100% to ~56%, Figure 2, inset). Such somewhat different "deactivation" behavior is understood when one considers that the former catalyst was screened at near full conversion level, i.e. the amount of catalyst sample was too large (always ~0.4 g). However, the turnover frequencies for both catalysts at final conversions (after 15–16 h of reaction) are similar (Table 3), so the apparent difference in the behavior of two 3 wt % Pd/MgO catalysts seen in Figure 2 is easily understood in terms of different metal particle sizes (7.9 vs. 15.6 nm), which differ by factor of ~2. For this metal particle range (~10 nm) one should not expect any special structure-sensitivity, which was usually observed for metal dispersions between

0.2 and 1 [47]. It must be emphasized that the final activity of MgF$_2$-supported Pd catalysts was higher than that previously obtained for Pd/Al$_2$O$_3$ [48] and active carbon-supported palladium [49,50] catalysts. This effect would speak for the beneficial effect of support acidity in electronic modification of palladium surface (creation of Pd$^{\sigma+}$ species).
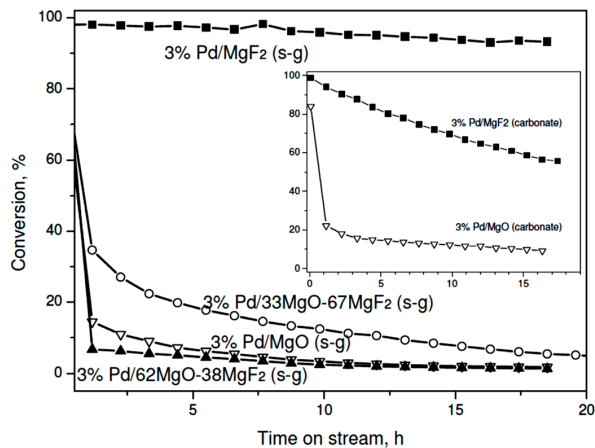
Figure 2. Time on stream behavior of 3 wt % Pd/MgO-MgF$_2$ (sol-gel) catalysts in CCl$_4$ hydrodechlorination at 90 °C. Inset: The behavior of the "carbonate" series of catalysts.

On the other hand, very different palladium dispersions in the sol-gel series prevent any speculation about a possible role of support in shaping the catalytic behavior. Therefore, it is concluded that palladium particle size of palladium, which is commonly considered as the catalytically active phase, must be a dominant factor. Thus, to investigate a possible role of support one needs to test palladium catalysts characterized by a similar metal dispersion. As mentioned earlier preparation of the carbonate series of 1 wt % Pd/MgO-MgF$_2$ catalysts, gave the catalysts characterized by similar metal particle sizes (~4 nm) (Table 2). Now the MgF$_2$-supported catalyst showed a poorer performance than its counterparts characterized by 3 wt % metal loading (Figure 3). Again, such effect would be ascribed to the metal particle size effect. Unexpectedly, the activity time on stream behavior of 1 wt % Pd/MgO was similar to that shown by 1 wt % Pd/MgF$_2$, although larger differences in product selectivity were found (next subsection). On the other hand, the MgO-MgF$_2$ supported catalyst showed an interesting behavior: For a longer time on stream the overall activity was higher and more stable than that for Pd/MgO and Pd/MgF$_2$. This effect will be discussed in the last part of discussion.
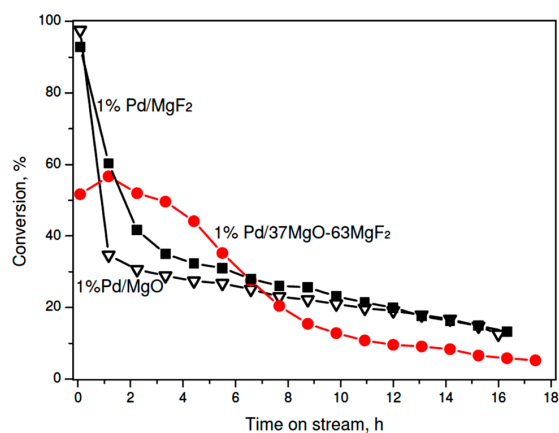
Figure 3. Time on stream behavior of 1 wt % Pd/MgO-MgF$_2$ (carbonate) catalysts in CCl$_4$ hydrodechlorination at 90 °C.

Table 3. CCl$_4$ hydrodechlorination on Pd/MgO-MgF$_2$ catalysts. Final conversions, product selectivities, TOFs and activation energies.

Catalyst	Final Conversion [a]	Product Distribution [a], %						TOF [b], s^{-1}	Activation Energy [c], kJ/mol
		CH$_4$	C$_2$-C$_5$	CH$_x$Cl$_{4x}$	C$_2$H$_x$Cl$_y$	C$_3$H$_x$Cl$_y$	ΣC$_1$-C$_5$		
Sol-Gel Series									
3% Pd/MgO	1.4	20.9	15.5	3.7	52.9	7.0	36.4	1.95×10^{-4}	56.7 ± 1.4
3% Pd/62% MgO-38% MgF$_2$	1.8	17.4	19.9	11.4	43.8	7.5	37.3	2.38×10^{-4}	50.0 ± 2.1
3% Pd/33% MgO-67% MgF$_2$	4.9	16.1	23.3	8.9	47.8	3.9	39.4	6.10×10^{-4}	51.3 ± 5.2
3% Pd/MgF$_2$	93.4	20.5	42.2	8.8	24.5	4.0	62.7	5.55×10^{-2}	38.3 ± 1.8
Carbonate Series									
3% Pd/MgO	9.5	16.9	25.9	11.8	38.8	6.6	42.8	1.57×10^{-3}	48.5 ± 4.6
3% Pd/MgF$_2$	56.1	23.9	35.1	15.9	20.5	4.6	59.0	5.36×10^{-2}	42.1 ± 1.3
1% Pd/MgO	13.7	17.0	10.6	7.8	62.9	1.6	27.7	2.15×10^{-2}	65.0 ± 6.2
1% Pd/37% MgO-63% MgF$_2$	5.5	26.6	22.6	3.5	40.8	6.5	49.2	5.08×10^{-3}	50.7 ± 5.6
1% Pd/MgF$_2$	14.1	20.6	32.9	15.9	26.3	4.3	53.5	1.51×10^{-2}	46.3 ± 5.7

[a] Final conversions and product selectivities after 15–16 h of time on stream (reaction temperature 90 °C); [b] Turnover frequency (at 90 °C) after 15–16 h of time on stream, based on dispersion data shown in Table 2 (CO/Pd); [c] Based on overall conversions collected at 70, 80 and 90 °C.

2.2.2. Product Selectivities and Activation Energies

We consider that chlorine-free compounds (i.e., hydrocarbons) are the desired products of CCl_4 hydrodechlorination because chloroform, a previously desired product, is classified as an extremely hazardous substance. In this respect all tested here MgF_2-supported palladium catalysts showed the best results, as indicated in Table 3, where one column aggregates C_2-C_5 hydrocarbon products. A higher activation energy for MgO-supported palladium would suggest that the removal of surface chlorine (as HCl) is more difficult than for the MgF_2-supported metal. This comparison clearly confirms the suitability of MgF_2-supported metal catalysts for HdCl reactions [14,20,21,24–26].

2.2.3. Working State of MgO-MgF_2 Supported Palladium Catalyst

The used samples of catalysts were investigated by XRD, temperature programmed hydrogenation of post-reaction deposits and IR spectroscopy of adsorbed pyridine (on selected samples). The results shown in Figures 4–8 and Table 4 allow to make cautious speculations about the working state of HdCl catalysts.

Table 4. Desorption of pyridine from 1 wt% Pd/MgO-MgF_2, 1 wt % Pd/MgF_2 and 3 wt % Pd/MgO catalysts. Absorbance (A) of 1446 cm^{-1} band (LPy) after desorption at different temperatures.

Catalyst Sample	T_{des}, °C	A	%A	A_{300}/A_{200}
1 % Pd/37MgO-63MgF$_2$ reduced	150	0.124	100.00	0.644
	200	0.082	66.13	
	250	0.059	47.58	
	300	0.0528	42.58	
1 % Pd/37MgO-63MgF$_2$ after HdCl	150	0.337	100.00	0.339
	200	0.096	28.49	
	250	0.0325	9.64	
	300	0.0254	7.54	
1 % Pd/MgF$_2$ after HdCl	150	0.0874	100.00	0.360
	200	0.0414	47.37	
	250	0.0237	27.12	
	300	0.0149	17.05	
3% Pd/MgO after HdCl	150	0.0049	100.00	0.251
	200	0.0045	91.84	
	250	0.00127	25.92	
	300	0.00113	23.06	

X-ray results (Figures 4 and 5) indicate that palladium, when it is detectable in the diffractograms, is largely transformed into a PdC_x phase. Such transformation is often observed for HdCl reactions carried out over Pd catalysts [49,51] and here confirmed for MgF_2-supported Pd catalyst used in the CCl_4 reaction. This phenomenon may decide about the time scale behavior of product selectivity pattern because at an initial period of reaction palladium acts as carbon sink decreasing the selectivity to methane [47,51].

Figures 4 and 5 showed big changes for the magnesium-containing support component. Direct transformation of MgO into $MgCl_2$ is also not unexpected, as a similar effect was observed for Pt/MgO catalyst by Choi et al. [20]. However, a closer inspection of diffractograms allows estimation of the extent of transformation and, hopefully, the state of crystallinity of formed $MgCl_2$. Figure 4 shows that magnesia in 3 wt % Pd/MgO catalyst is only partly transformed into $MgCl_2$. In MgO-MgF_2 supported 3% Pd loaded catalysts the extent of transformation appears more marked. Figure 5 shows analogous data for the carbonate series of Pd catalysts. Here the degree of MgO → $MgCl_2$ transformation is still more pronounced. For the 1 wt % loaded catalysts the presence of $MgCl_2$ and MgO phases is only slightly marked (for 1 wt % Pd/MgO) or even completely invisible for 1 wt % Pd/37MgO-63MgF$_2$

catalyst. These observations along with much broader reflections from the $MgCl_2$ in the 3 wt % Pd/MgO catalyst that the formed $MgCl_2$ phase has a tendency to spread out over the catalyst surface.
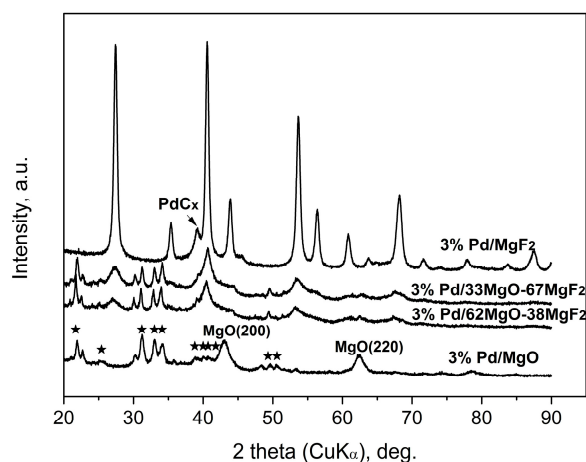

Figure 4. XRD profiles of 3 wt % Pd/MgO-MgF_2(sol-gel) catalysts after CCl_4 hydrodechlorination. The five-pointed stars show the main reflections of $MgCl_2 \cdot 6H_2O$ (PDF #760789).
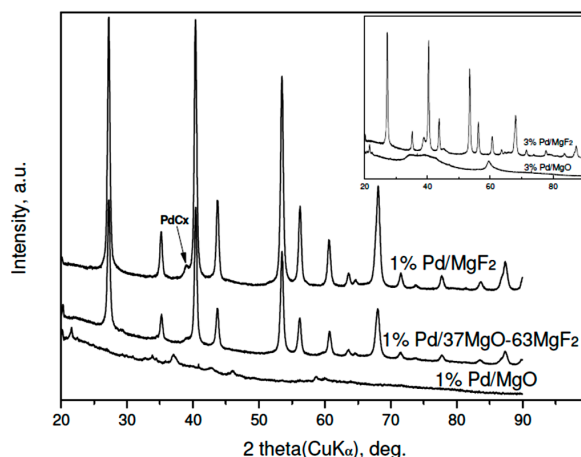

Figure 5. XRD profiles of Pd/MgO-MgF_2(carbonate) catalysts after CCl_4 hydrodechlorination.

Temperature programed hydrogenation of post-reaction deposits presented in Figures 6 and 7 shows that all tested catalysts possess different amounts of carbon and chlorine. MgF_2-supported catalysts are relatively deprived of chlorine: only some small amount of HCl is liberated at low temperature ($\leq$200 °C), suggesting reduction of chloride associated with the palladium. A nonappearance of high temperature HCl evolution (observed for MgO-containing catalysts) indicates lack of chlorine on the surface of MgF_2 (Figure 7). This, in turn, suggests no changes in the acidity of this catalyst which would be associated with chlorine. However, CH_4 evolution from this catalyst was quite pronounced (Figure 6) but still not as high as for other catalysts, which we believe is a primary reason of catalyst deactivation in HdCl reactions. Interestingly, Figure 7 shows no chlorine liberation for Pd/MgO at a low temperature region. We believe that it is not due to a lack of chlorine on palladium surface but rather because the surface of palladium is effectively blocked by an impermeable coating by $MgCl_2$, [52] or simply closed in a porous structure by $MgCl_2$ "stoppers". As it was suggested earlier, a decreased crystallinity of $MgCl_2$ in this catalyst allows assumption that $MgCl_2$ is either spread out over the support or a topochemical reaction MgO-$MgCl_2$ [52] would lead to dramatic changes in the support texture, with possible burial of Pd particles. The MgO-MgF_2 supported catalysts showed both the low and high temperature HCl evolution, evidencing that both $MgCl_2$ spreading as well as textural

changes would be less dramatic for mixed MgO-MgF$_2$ systems, where a part of palladium species is deposited on MgF$_2$. It looks like the very huge HCl evolution from Pd/MgO occurred at very high temperature largely results from reduction of MgCl$_2$.
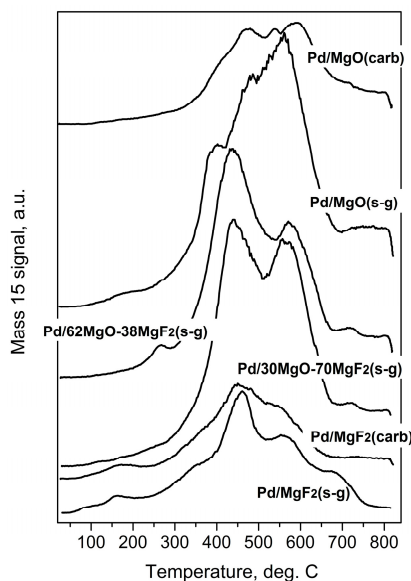

Figure 6. Temperature programmed hydrogenation of post-reaction deposits from Pd/MgO-MgF$_2$ catalysts. Mass 15 was selected for monitoring methane evolution because mass 16 would also reflect the signal from water.
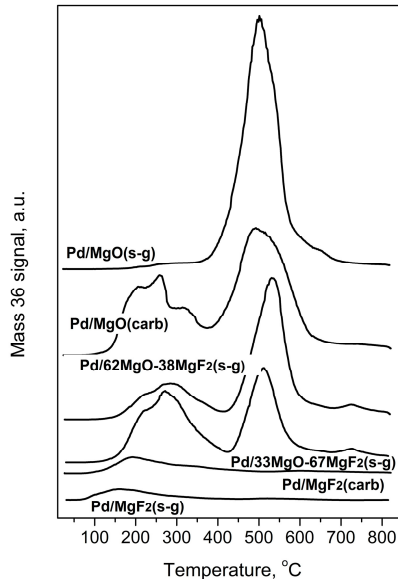
Figure 7. Evolution of HCl during Temperature Programmed Hydrogenation of post-reaction deposits from Pd/MgO-MgF$_2$ catalysts.

The results of IR spectra of adsorbed pyridine (Figure 8a,b and Table 4) allow to confirm the presence of Lewis acid centers on the surface of all tested catalysts. The analysis of population and strength distribution of these centers was carried out by considering the absorbance of 1446 cm^{-1} band, associated with pyridine coordinated to the Lewis acid center. The largest amounts of pyridine left on the surface after desorption at 150 °C were found for used 1 wt % Pd/37MgO-67MgF$_2$ catalyst. The number of such centers was nearly three times higher than the respective value for the reduced

catalyst. However, these centers are rather weak because after desorption at 200 °C only 28.5% of them still bind pyridine. On the other hand, at analogous conditions, as far as 66% of pyridine is left on the reduced catalyst. A quantitative parameter characterizing the strength of acid centers is the ratio of the 1446 cm^{-1} absorbance after pyridine desorption at 300 and 200 °C. Table 4 displays that the highest value of this parameter (0.64) showed the reduced 1 wt % Pd/37MgO-67MgF$_2$ catalyst, whereas after HdCl it decreased to 0.26. A similar value was found for 1 wt % Pd/MgO after reaction (0.25). Therefore, it appears that during the HdCl reaction the strongest acid centers are neutralized with simultaneous formation of weak acid centers. It would be worthwile to investigate the acid strength evolution in the course of reaction and combine it with the catalytic performance (activity and selectivity).
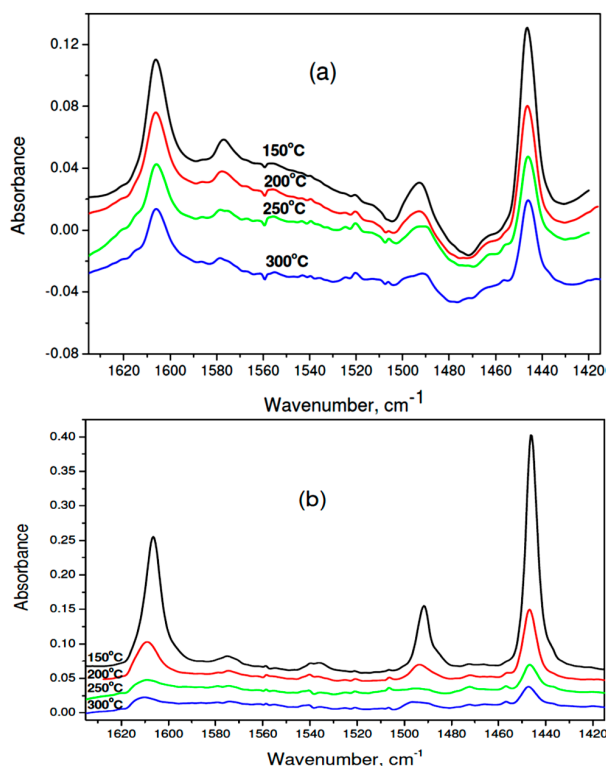
Figure 8. IR spectra of adsorbed pyridine on 1 wt % Pd/37MgO-63MgF$_2$ catalyst: (**a**) after reduction, (**b**) after CCl$_4$ hydrodechlorination. Numbers ascribed to spectra indicate the temperature of pyridine desorption.

In summary, the role of support acidity is quite complex. On the one hand, a definite, although not very high Lewis acidity of MgF$_2$ is beneficial for shaping high activity of palladium catalysts. The MgO-MgF$_2$ support characterized by stronger Lewis acidity than MgF$_2$ contributes to very good catalytic activity for a relatively long reaction period (~5 h) but subsequent neutralization of stronger acid centers (by coking) eliminates them from the catalytic amphitheater. On the other hand, the role of acidity evolution, which takes place when basic supports (like MgO) are chlorided during HdCl reactions, is difficult to assess because different events associated with distribution of chlorided support species, leading to partial or even full blocking of the surface of palladium, which plays the role of active phase in HdCl reactions. Therefore, a unique disposal of straightforward tuneability of acido-basic properties of MgO-MgF$_2$ of varied composition is weakened by the interaction with chloride species. It must recalled that these sites, tuned over a wide range of MgO-MgF$_2$ composition, gave an unproblematic access to optimized catalytic activity and selectivity of these phases for the Michael addition of 2-methylcyclohexane-1,3-dione to methyl vinyl ketone [31]. By increasing the fluorine content of the magnesium oxide fluoride, the Lewis acidity increases whereas the basicity

decreases [30]. This correlation is also compatible with recent results on toluene hydrogenation over Ir/MgO-MgF$_2$ catalysts [53], where the best iridium catalysts were supported on MgF$_2$-rich carriers characterized by a relatively low surface basicity.

3. Experimental Section

3.1. Preparation of MgO-MgF$_2$ Supports

Two series of MgO-MgF$_2$ supports were prepared. The first one was synthesized by the sol-gel method starting from magnesium methoxide treated with an aqueous solution of hydrofluoric acid, as described in [32]. The amount of HF solution was adjusted to obtain 40 and 70 mol % MgF$_2$ in the samples. The resulting dense gels of MgO-MgF$_2$ were subjected to ageing for 40 h at RT, and then to drying at 80 °C for 3 h. The dried samples of this "sol-gel" series were calcined for 4 h at 400 °C and sieved (selected fraction 0.25–0.5 mm). The MgF$_2$ support was obtained by the sol-gel method from Mg(OCH$_3$)$_2$ and anhydrous HF (48.8% HF in methanol, Sigma-Aldrich, Polska, Poznań, Poland) in a way analogous to the above described synthesis for MgO-MgF$_2$, but under rigorously anhydrous conditions. MgO was obtained by the sol-gel method by hydrolysis of magnesium methoxide (120 cm^3 of 0.5 M solution) in water and treated similarly to MgO-MgF$_2$. Another series of MgO-MgF$_2$ supports of different MgF$_2$ contents (0, 60% and 100%) were obtained in the reaction of basic magnesium carbonate (4MgCO$_3$·Mg(OH)$_2$·5H$_2$O) powder with controlled amounts of 40 wt % aqueous solution of HF, as described in [33]. The resulting dense gels of this "carbonate" series were aged for 40 h at room temperature under stirring, followed by drying at 80 °C for 24 h and calcining under air flow at 500 °C for 4 h. The MgO support was obtained by decomposition of 4MgCO$_3$·Mg(OH)$_2$·5H$_2$O at 500 °C for 4 h.

3.2. Preparation of MgO-MgF$_2$ Supported Palladium Catalysts

The 3 wt % Pd/MgO-MgF$_2$ catalysts were prepared by impregnation of both series of MgO-MgF$_2$ supports with an acetone solution of palladium acetate using the incipient wetness technique. The 1 wt % Pd-loaded catalysts were prepared by wet impregnation of the "carbonate" supports with a methanol solution of palladium acetate. After impregnation and drying (at 80 °C for 20 h), the resulting solids were transferred to glass-stoppered bottles and kept in a desiccator. Prior to chemisorption and reaction studies, all catalysts were reduced in flowing 20% H$_2$/Ar (50 cm^3/min), ramping the temperature from 20 to 380 °C (at 8 °C/min), and kept at 380 °C for 2 h.

3.3. Characterization of Catalysts

The catalysts were characterized by H$_2$ and CO chemisorption, XRD, temperature-programmed methods and IR spectroscopy of adsorbed pyridine. Irreversible uptake of hydrogen was measured in a pulse method system at 70 °C, to avoid the formation of β-PdH. CO adsorption was measured at 35 °C in a static system, using a double isotherm method (ASAP 2020 from Micromeritics). H$_{ad}$/Pd and CO$_{ad}$/Pd ratios were taken as measures of metal dispersion. Prior to characterization, the catalysts were pretreated in the same way as before kinetic experiments (next subsection), i.e., with the final reduction at 380 °C for 2 h. Reduced and post-reaction catalysts were investigated by X-ray diffractometry (PANalytical Empyrean, Almelo, The Netherlands, with Ni-filtered CuK$_\alpha$ radiation and sample spinner).

After H$_2$ chemisorption, the samples were cooled to room temperature and subjected to a temperature programmed study in 10% H$_2$/Ar flow, ramping the temperature from 20 to 150 °C, at 8 °C/min. Since the samples had already been reduced, the aim of such experiments was to monitor hydrogen evolution during decomposition of Pd hydride, in the temperature programmed hydride decomposition (TPHD). For details, see [34]. Post-reaction catalyst samples were investigated by temperature programmed hydrogenation (TPH-MS). TPH-MS runs were carried out in a flowing

10% H_2/He mixture (25 cm^3/min) at a 10 °C/min ramp and followed by mass spectrometry (MA200 Dycor-Ametek, Pittsburgh, PA, USA). For details, see [49].

The FTIR spectra of adsorbed pyridine were collected using a Thermo Scientific Nicolet 6700 (Madison, WI, USA) equipped with a MTC-A detector in transmission mode with a spectral resolution 4 cm^{-1}. The OMNIC software (version 7.3, Thermo Electron Corporation, Madison, WI, USA) was used to collect and analyze spectra of adsorbed pyridine on selected (mainly post-reaction) catalysts samples which, after crushing, were pressed into self-supporting pellets of 18 mm diameter and mass ~20 mg. Prior to adsorption the sample was outgassed at 350 °C down to 10^{-5} mbar for 5 h. Then, it was cooled to room temperature and the IR spectrum was collected. Next, the sample was heated to 150 °C and contacted with pyridine vapor (dried over KOH, distilled and outgassed) for 10 min and pyridine desorption was carried out for 30 min. After collecting the spectrum, the temperature was gradually raised by 50 °C. In this way spectra of adsorbed pyridine at 200, 250 and 300 °C were collected and analyzed after subtracting background measured before pyridine adsorption.

3.4. Hydrodechlorination of Tetrachloromethane

Prior to the reaction, the catalyst charge (~0.4 g) was dried at 120 °C for 0.5 h in an argon flow and reduced in flowing 20% H_2/Ar (25 cm^3/min), ramping the temperature from 120 °C to 380 °C (at 8 °C/min) and kept at 380 °C for 2 h. The reaction of HdCl of tetrachloromethane was carried out at 90 °C, the H_2:CCl$_4$ ratio ~14:1 and total flow 29 cm^3/min, in a glass flow system, as previously described [50]. The partial pressures of the reaction mixture were: CCl$_4$ 4.3 kPa, H_2 60.5 kPa, Ar 36.5 kPa. The reaction (at 90 °C) was followed by gas chromatography. After catalyst screening at 90 °C and reaching a nearly constant conversion, the temperature was gradually decreased to 80 °C and 70 °C, and new experimental points were collected. Finally, the reactor was heated to 90 °C, and, in nearly all cases, the previous results collected at 90 °C were restored. A typical run lasted~20 h.

References

1. Kovalchuk, V.I.; d'Itri, J.L. Catalytic chemistry of chloro- and chlorofluorocarbon dehalogenation: From macroscopic observations to molecular level understanding. *Appl. Catal. A Gen.* **2004**, *271*, 13–25. [CrossRef]

2. Keane, M.A. Supported Transition Metal Catalysts for Hydrodechlorination Reactions. *ChemCatChem* **2011**, *3*, 800–821. [CrossRef]

3. Zhang, Z.C.; Beard, B.C. Genesis of durable catalyst for selective hydrodechlorination of CCl$_4$ to CHCl$_3$. *Appl. Catal. A* **1998**, *174*, 33–39. [CrossRef]

4. Coq, B.; Cognion, J.-M.; Figuéras, F.; Tournigant, D. Conversion Under Hydrogen of Dichlorodifluoromethane over Supported Palladium Catalysts. *J. Catal.* **1993**, *141*, 21–33. [CrossRef]

5. Coq, B.; Figuéras, F.; Hub, S.; Tournigant, D. Effect of the Metal-Support Interaction on the Catalytic Properties of Palladium for the Conversion of Difluorodichloromethane with Hydrogen: Comparison of Oxides and Fluorides as Supports. *J. Phys. Chem.* **1995**, *99*, 11159–11166. [CrossRef]

6. Colombo, A.; Dragonetti, C.; Magni, M.; Roberto, D. Degradation of toxic halogenated organic compounds by iron-containing mono-, bi- and tri-metallic particles in water. *Inorg. Chim. Acta* **2015**, *431*, 48–60. [CrossRef]

7. Berndt, H.; Bozorg Zadeh, H.; Kemnitz, E.; Nickkho-Amiry, M.; Pohl, M.; Skapin, T.; Winfield, J.M. The properties of platinum or palladium supported on β-aluminium trifluoride or magnesium difluoride: Catalysts for the hydrodechlorination of 1,1-dichlorotetrafluoroethane. *J. Mater. Chem.* **2002**, *12*, 3499–3507. [CrossRef]

8. Stakheev, A.Y.; Sachtler, W.M.H. Determination by X-ray photoelectron spectroscopy of the electronic state of Pd clusters in Y zeolite. *J. Chem. Soc. Faraday Trans.* **1991**, *87*, 3703–3708. [CrossRef]

9. Coq, B.; Medina, F.; Tichit, D.; Morato, A. The catalytic transformation of chlorofluorocarbons in hydrogen on metal-based catalysts supported on inorganic fluorides. *Catal. Today* **2004**, *88*, 127–137. [CrossRef]

10. Martin-Martinez, M.; Gómez-Sainero, L.M.; Bedia, J.; Arevalo-Bastante, A.; Rodriguez, J.J. Enhanced activity of carbon-supported Pd–Pt catalysts in the hydrodechlorination of dichloromethane. *Appl. Catal. B* **2016**, *184*, 55–63. [CrossRef]

11. Diaz, E.; Mohedano, A.F.; Casas, J.A.; Shalaby, C.; Eser, S.; Rodriguez, J.J. On the performance of Pd and Rh catalysts over different supports in the hydrodechlorination of the MCPA herbicide. *Appl. Catal. B* **2016**, *186*, 151–156. [CrossRef]

12. Alvarez-Montero, M.A.; Gomez-Sainero, L.M.; Martin-Martinez, M.; Heras, F.; Rodriguez, J.J. Hydrodechlorination of chloromethanes with Pd on activated carbon catalysts for the treatment of residual gas streams. *Appl. Catal. B* **2010**, *96*, 148–156. [CrossRef]

13. Gomez-Sainero, L.M.; Seoane, X.L.; Fierro, J.L.G.; Arcoya, A. Liquid-Phase Hydrodechlorination of CCl_4 to $CHCl_3$ on Pd/Carbon Catalysts: Nature and Role of Pd Active Species. *J. Catal.* **2002**, *209*, 279–288. [CrossRef]

14. Babu, N.S.; Lingaiah, N.; Pasha, N.; Kumar, J.V.; Prasad, P.S.S. Influence of particle size and nature of Pd species on the hydrodechlorination of chloroaromatics: Studies on Pd/TiO_2 catalysts in chlorobenzene conversion. *Catal. Today* **2009**, *141*, 120–124. [CrossRef]

15. Ding, E.; Jujjuri, S.; Sturgeon, M.; Shore, S.G.; Keane, M.A. Novel one step preparation of silica supported Pd/Sr and Pd/Ba catalysts via an organometallic precursor: Application in hydrodechlorination and hydrogenation. *J. Mol. Catal. A* **2008**, *294*, 51–60. [CrossRef]

16. Cobo, M.I.; Conesa, J.A.; de Correa, C.M. The Effect of NaOH on the Liquid-Phase Hydrodechlorination of Dioxins over Pd/γ-Al_2O_3. *J. Phys. Chem. A* **2008**, *112*, 8715–8722. [CrossRef] [PubMed]

17. Jujjuri, S.; Ding, E.; Hommel, E.L.; Shore, S.G.; Keane, M.A. Synthesis and characterization of novel silica-supported Pd/Yb bimetallic catalysts: Application in gas-phase hydrodechlorination and hydrogenation. *J. Catal.* **2006**, *239*, 486–500. [CrossRef]

18. Early, K.; Kovalchuk, V.I.; Lonyi, F.; Deshmukh, S.; d'Itri, J.L. Hydrodechlorination of 1,1-Dichlorotetrafluoroethane and Dichlorodifluoromethane Catalyzed by Pd on Fluorinated Aluminas: The Role of Support Material. *J. Catal.* **1999**, *182*, 219–227. [CrossRef]

19. Álvarez-Montero, M.A.; Rodriguez, J.J.; Gómez-Sainero, L.M. Platinum Nanoparticles Supported on Activated Carbon Catalysts for the Gas-phase Hydrodechlorination of Dichloromethane: Influence of Catalyst Composition and Operating Conditions. *Nanomater. Nanotechnol.* **2016**, *6*, 18. [CrossRef]

20. Choi, H.C.; Choi, S.H.; Yang, O.B.; Lee, J.S.; Lee, K.H.; Kim, Y.G. Hydrodechlorination of Carbon Tetrachloride over Pt/MgO. *J. Catal.* **1996**, *161*, 790–797. [CrossRef]

21. Dal Santo, V.; Dossi, C.; Recchia, S.; Colavita, P.E.; Vlaic, G.; Psaro, R. Carbon tetrachloride hydrodechlorination with organometallics-based platinum and palladium catalysts on MgO. *J. Mol. Catal. A* **2002**, *182–183*, 157–166. [CrossRef]

22. Aytam, H.P.; Akula, V.; Janmanchi, K.; Kamaraju, S.R.R.; Panja, K.R.; Gurram, K.; Niemantsverdriet, J.W. Characterization and Reactivity of Pd/MgO and Pd/γ-Al_2O_3 Catalysts in the Selective Hydrogenolysis of CCl_2F_2. *J. Phys. Chem. B* **2002**, *106*, 1024–1031. [CrossRef]

23. Clarke, J.K.A.; Bradley, M.I.; Garvie, L.A.J.; Craven, A.J.; Baird, T. Pt/MgO as Catalyst for Hydrogenolysis Reactions of C_5 and C_6 Hydrocarbons: Evidence for Metal-Support Interactions. *J. Catal.* **1993**, *143*, 122–137. [CrossRef]

24. Padmasri, A.H.; Venugopal, A.; Siva Kumar, V.; Shashikala, V.; Nagaraja, B.M.; Seetharamulu, P.; Sreedhar, B.; David Raju, B.; Kanta Rao, P.; Rama Rao, K.S. Role of hydrotalcite precursors as supports for Pd catalysts in hydrodechlorination of CCl_2F_2. *J. Mol. Catal. A* **2004**, *223*, 329–337. [CrossRef]

25. Malinowski, A.; Juszczyk, W.; Pielaszek, J.; Bonarowska, M.; Wojciechowska, M.; Karpiński, Z. Magnesium fluoride as a catalytic support in hydrodechlorination of CCl$_2$F$_2$ (CFC-12). *Chem. Commun.* **1999**, 685–686. [CrossRef]

26. Patil, P.T.; Dimitrov, A.; Kirmse, H.; Neumann, W.; Kemnitz, E. Non-aqueous sol–gel synthesis, characterization and catalytic properties of metal fluoride supported palladium nanoparticles. *Appl. Catal. B* **2008**, *78*, 80–91. [CrossRef]

27. Cao, Y.C.; Jiang, X.Z. Supported platinum–gallium catalysts for selective hydrodechlorination of CCl$_4$. *J. Mol. Catal. A* **2005**, *242*, 119–128. [CrossRef]

28. Cao, Y.C.; Li, Y. In situ synthesis of supported palladium complexes: Highly stable and selective supported palladium catalysts for hydrodechlorination of CCl$_2$F$_2$. *Appl. Catal. A* **2005**, *294*, 298–305. [CrossRef]

29. Murthy, J.K.; Chandra Shekar, S.; Padmasri, A.H.; Venugopal, A.; Siva Kumar, V.; Nagaraja, B.M.; Shashikala, V.; David Raju, B.; Kanta Rao, P.; Rama Rao, K.S. Promotional effect of magnesia addition to active carbon supported Pd catalyst on the characteristics and hydrodechlorination activity of CCl$_2$F$_2$. *Catal. Commun.* **2004**, *5*, 161–167. [CrossRef]

30. Wuttke, S.; Coman, S.M.; Kröhnert, J.; Jentoft, F.C.; Kemnitz, E. Sol–gel prepared nanoscopic metal fluorides—A new class of tunable acid–base catalysts. *Catal. Today* **2010**, *152*, 2–10. [CrossRef]

31. Prescott, H.A.; Li, Z.-J.; Kemnitz, E.; Deutsch, J.; Lieske, H. New magnesium oxide fluorides with hydroxy groups as catalysts for Michael additions. *J. Mater. Chem.* **2005**, *15*, 4616–4628. [CrossRef]

32. Zieliński, M.; Wojciechowska, M. Preparation of MgF$_2$-MgO supports with specified acid-base properties, and their influence on nickel catalyst activity in toluene hydrogenation. *Stud. Surf. Sci. Catal.* **2010**, *175*, 429–432.

33. Zieliński, M. The catalytic and physico-chemical properties of Ni/MgF$_2$–MgO catalysts. *Appl. Catal. A* **2012**, *449*, 15–22. [CrossRef]

34. Bonarowska, M.; Pielaszek, J.; Juszczyk, W.; Karpiński, Z. Characterization of Pd–Au/SiO$_2$ Catalysts by X-ray Diffraction, Temperature-Programmed Hydride Decomposition, and Catalytic Probes. *J. Catal.* **2000**, *195*, 304–315. [CrossRef]

35. Pinna, F.; Signoretto, M.; Strukul, I.G.; Polizzi, S.; Pernicone, N. Pd-SiO$_2$ catalysts. stability of β-PdHx as a function of Pd dispersion. *React. Kinet. Catal. Lett.* **1997**, *60*, 9–13. [CrossRef]

36. Nag, N.K. A Study on the Formation of Palladium Hydride in a Carbon-Supported Palladium Catalyst. *J. Phys. Chem. B* **2001**, *105*, 5945–5949. [CrossRef]

37. Ichikawa, S.; Poppa, H.; Boudart, M. Disproportionation of CO on small particles of silica-supported palladium. *J. Catal.* **1985**, *91*, 1–10. [CrossRef]

38. Zhang, Z.C.; Beard, B.C. Agglomeration of Pt particles in the presence of chlorides. *Appl. Catal. A* **1998**, *188*, 229–240. [CrossRef]

39. Bae, J.W.; Kim, I.G.; Lee, J.S.; Lee, K.H.; Jang, E.J. Hydrodechlorination of CCl4 over Pt/Al$_2$O$_3$: Effects of platinum particle size on product distribution. *Appl. Catal. A* **2003**, *240*, 129–142. [CrossRef]

40. Bae, J.W.; Lee, J.S.; Lee, K.H. Hydrodechlorination of CCl4 over Pt/γ-Al$_2$O$_3$ prepared from different Pt precursors. *Appl. Catal. A* **2008**, *334*, 156–167. [CrossRef]

41. Shin, E.-J.; Spiller, A.; Tavoularis, G.; Keane, M.A. Chlorine–nickel interactions in gas phase catalytic hydrodechlorination: Catalyst deactivation and the nature of reactive hydrogen. *Phys. Chem. Chem. Phys.* **1999**, *1*, 3173–3181. [CrossRef]

42. Ordonez, S.; Díez, F.V.; Sastre, H. Characterisation of the deactivation of platinum and palladium supported on activated carbon used as hydrodechlorination catalysts. *Appl. Catal. B* **2001**, *31*, 113–122. [CrossRef]

43. Frankel, K.A.; Jang, B.W.-L.; Spivey, J.J.; Roberts, G.W. Deactivation of hydrodechlorination catalysts: I. Experiments with 1,1,1-trichloroethane. *Appl. Catal. A* **2001**, *205*, 263–278. [CrossRef]

44. Frankel, K.A.; Jang, B.W.-L.; Roberts, G.W.; Spivey, J.J. Deactivation of hydrodechlorination catalysts: II—Experiments with 1,1-dichloroethylene and 1,1-dichloroethane. *Appl. Catal. A* **2001**, *209*, 401–413. [CrossRef]

45. Kim, S.Y.; Choi, H.C.; Yang, O.B.; Lee, K.H.; Lee, J.C.; Kim, J.G. Hydrodechlorination of tetrachloromethane over supported Pt catalysts. *J. Chem. Soc. Chem. Commun.* **1995**, 2169–2170. [CrossRef]

46. Legawiec-Jarzyna, M.; Śrębowata, A.; Juszczyk, W.; Karpiński, Z. Hydrodechlorination over Pd–Pt/Al$_2$O$_3$ catalysts: A comparative study of chlorine removal from dichlorodifluoromethane, carbon tetrachloride and 1,2-dichloroethane. *Appl. Catal. A* **2004**, *271*, 61–68. [CrossRef]

47. Bonarowska, M.; Kaszkur, Z.; Łomot, D.; Rawski, M.; Karpiński, Z. Effect of gold on catalytic behavior of palladium catalysts in hydrodechlorination of tetrachloromethane. *Appl. Catal. B* **2015**, *162*, 45–56. [CrossRef]

48. Moon, D.J.; Chung, M.J.; Park, K.Y.; Hong, S.I. Deactivation of Pd catalysts in the hydrodechlorination of chloropentafluoroethane. *Appl. Catal. A* **1998**, *168*, 159–170. [CrossRef]

49. Juszczyk, W.; Malinowski, A.; Karpiński, Z. Hydrodechlorination of CCl_2F_2 (CFC-12) over γ-alumina supported palladium catalysts. *Appl. Catal. A* **1998**, *166*, 311–319. [CrossRef]

50. Bonarowska, M.; Karpiński, Z.; Kosydar, R.; Szumełda, T.; Drelinkiewicz, A. Hydrodechlorination of CCl_4 over carbon-supported palladium–gold catalysts prepared by the reverse "water-in-oil" microemulsion method. *C. R. Chim.* **2015**, *18*, 1143–1151. [CrossRef]

51. Bonarowska, M.; Kaszkur, Z.; Słowik, G.; Ryczkowski, J.; Karpiński, Z. Tetrachloromethane as an Effective Agent to Transform Nanoparticles of Palladium and Gold in Supported Catalysts. *ChemCatChem* **2016**, *8*, 2625–2629. [CrossRef]

52. Fenelonov, V.B.; Mel'gunov, M.S.; Mishakov, I.V.; Richards, R.M.; Chesnokov, V.V.; Volodin, A.M.; Klabunde, K.J. Changes in Texture and Catalytic Activity of Nanocrystalline MgO during Its Transformation to $MgCl_2$ in the Reaction with 1-Chlorobutane. *J. Phys. Chem. B* **2001**, *105*, 3937–3941. [CrossRef]

53. Zieliński, M.; Kiderys, A.; Pietrowski, M.; Tomska-Foralewska, I.; Wojciechowska, M. Synthesis and characterization of new Mg–O–F system and its application as catalytic support. *Catal. Commun.* **2016**, *76*, 54–57. [CrossRef]

Sample Availability: Samples of the catalysts and supports are not available from the authors.